RESEARCH ARTICLE

Effect of sevoflurane preconditioning on astrocytic dynamics and neural network formation after cerebral ischemia and reperfusion in rats

Qiong Yu[#], Li Li[#], Wei-Min Liang[*]
Department of Anesthesiology, Huashan Hospital, Fudan University, Shanghai, China

Funding: *This study was supported by the National Natural Science Foundation of China, No. 81200937 (to QY).*

Graphical Abstract

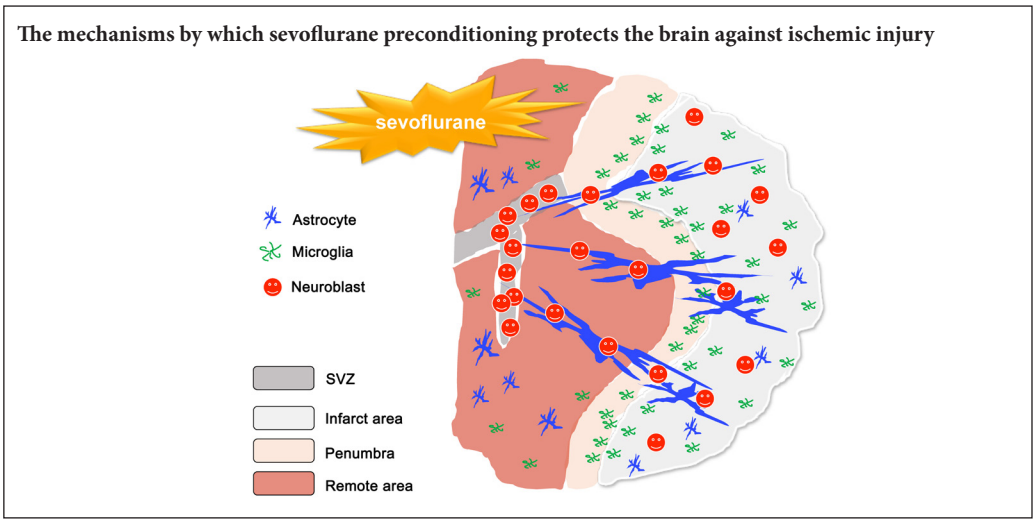

Correspondence to:
Wei-Min Liang, MD, PhD, chiefliang@sina.cn.

#These authors contributed equally to this work.

orcid:
0000-0002-4484-7225 (Wei-Min Liang)

doi: *10.4103/1673-5374.244790*

Received: *March 7, 2018*
Accepted: *September 11, 2018*

Abstract

Astrocytes, the major component of blood-brain barriers, have presented paradoxical profiles after cerebral ischemia and reperfusion *in vivo* and *in vitro*. Our previous study showed that sevoflurane preconditioning improved the integrity of blood-brain barriers after ischemia and reperfusion injury in rats. This led us to investigate the effects of sevoflurane preconditioning on the astrocytic dynamics in ischemia and reperfusion rats, in order to explore astrocytic cell-based mechanisms of sevoflurane preconditioning. In the present study, 2,3,5-triphenyltetrazolium chloride staining and Garcia behavioral scores were utilized to evaluate cerebral infarction and neurological outcome from day 1 to day 3 after transient middle cerebral artery occlusion surgery. Using immunofluorescent staining, we found that sevoflurane preconditioning substantially promoted the astrocytic activation and migration from the penumbra to the infarct with microglial activation from day 3 after middle cerebral artery occlusion. The formation of astrocytic scaffolds facilitated neuroblasts migrating from the subventricular zone to the lesion sites on day 14 after injury. Neural networks increased in the infarct of sevoflurane preconditioned rats, consistent with decreased infarct volume and improved neurological scores after ischemia and reperfusion injury. These findings demonstrate that sevoflurane preconditioning confers neuroprotection, not only by accelerating astrocytic spatial and temporal dynamics, but also providing astrocytic scaffolds for neuroblasts migration to ischemic regions, which facilitates neural reconstruction after brain ischemia.

Key Words: *nerve regeneration; sevoflurane; ischemia and reperfusion; neuroprotection; astrocytes; dynamics; neuroblast; glial scar; neural network; stroke; inhalational anesthetics; neural regeneration*

Chinese Library Classification No. *R453; R361; R741*

Introduction

Stroke is the primary leading cause of death in China with an increasing morbidity rate of 8.7% per year since 1986 (Wang et al., 2017), which results in profound physiological and emotional burdens on survivors, and enormous social consequences. It has been reported that some neurosurgical, vascular and cardiovascular procedures present a high risk for transient focal cerebral ischemia (Arrowsmith et al., 2000; Wilson et al., 2005). Sevoflurane (2–4%), a commonly used inhalational anesthetic, is routinely used for moderate to deep sedation during surgeries. Recent studies showed that 1.2–4% sevoflurane could effectively prevent the brain against cerebral ischemia and reperfusion (I/R) in rodents *in vivo* and *in vitro* (Yu et al., 2010; Chen et al., 2015; Zhang et al., 2015). However, the protective mechanism remains unclear. Our previous studies found that repeated sevoflurane preconditioning reduced blood-brain barrier leakage (Yu et al., 2011). It also suppressed the expression of nuclear factor-kappa B and downstream inflammatory cytokines in rats after transient middle cerebral artery occlusion (tMCAO) (Wang et al.,

2011), indicating an anti-inflammatory role for sevoflurane in preconditioning against brain ischemia.

Astrocytes, an essential component of blood-brain barriers, present paradoxical profiles at early and late stages after stroke (Maki et al., 2013; Han et al., 2018). Reactive astrocytes aggravate the inflammatory response by releasing pro-inflammatory cytokines and apoptotic messengers to healthy regions in the acute phases (Anderson et al., 2003; Sofroniew and Vinters, 2010; Ologunde and Ma, 2011). On the other hand, astrocytes limit the spreading of ischemic lesions by building glial scars and release neurotrophins for brain recovery (Liu and Chopp, 2016). Based on our previous results, we put forward the hypothesis that astrocytes might contribute to the sevoflurane-induced neuroprotection. The astrocytic dynamic changes by sevoflurane preconditioning might provide information for potential therapeutic strategies in human stroke. In the current study, we used immunostaining to investigate the effects of sevoflurane preconditioning on astrocytic temporospatial dynamics and the formation of neural networks for 28 days after brain I/R injury.

Materials and Methods

Animals

Adult male Sprague-Dawley rats weighing 280–320 g were purchased from the SLAC Laboratory Animal Co., Ltd. (Shanghai, China). The rats were randomly divided into three groups: the sham (n = 25), ischemia (ischemic exposure only, n = 56) and sevoflurane (Sevo) groups (Sevo-preconditioned + ischemic exposure, n = 54). A total of 135 rats were used in the current study. All procedures were approved by the Animal Ethics Committee of Fudan University, China (2017 Huashan Hospital JS-003) on January 4, 2017 and performed in accordance with the National Institutes of Health Guide for the Care and Use of Laboratory Animals (NIH Publication No. 85-23, revised 1996), and approved by the Animal Ethics Committee of Fudan University, China (2017 Huashan Hospital JS-003) on January 4, 2017.

tMCAO and treatment

Right tMCAO was carried out to mimic focal cerebral I/R injury as described previously (Wang et al., 2005; Li et al., 2017). Briefly, the rats were intraperitoneally anesthetized with 40 mg/kg ketamine (Libang Pharmaceutical Co., Ltd., Xi'an, China) and allowed to breathe spontaneously. After the right common carotid artery was ligated proximally, a monofilament (Sunbio Biotech Co., Ltd., Beijing, China) with a diameter of 0.38 ± 0.02 mm was inserted through an arteriectomy in the right common carotid artery, just below the carotid bifurcation, and advanced gently along the internal carotid artery up to the origin of the right middle cerebral artery. After 90-minute brain ischemia, the monofilament was withdrawn to allow reperfusion of the right middle cerebral artery territory. Throughout the surgery, the body temperature was maintained at 37 ± 0.2°C with a heating pad. After recovery from anesthesia, the rats were placed back into their cages with free access to food and water.

In the Sevo group, rats were exposed to 1.2% sevoflurane (Baxter, Baxter Health Ltd., Norfolk, UK) + 98% O_2 in an anesthetic chamber (Baxter Health Ltd.) for 60 minutes once per day for 4 consecutive days as described previously (Yu et al., 2011; Li et al., 2017). The rats in the ischemia group were exposed to 98% O_2 instead. After 24 hours of 4-day treatment, the rats of the ischemia and Sevo groups were subjected to tMCAO. The rats of the sham group were neither exposed to sevoflurane nor had ischemia induced. In accordance with our previous study, the successful rate of tMCAO modelling was 0.86 (Li et al., 2017). Successful modelling after 90 minutes of cerebral ischemia was identified by the rats' motor deficits, including the flexor positions of the left front limbs and continuous circling due to locomotive disturbance. The rats with a hemorrhage or without an infarct were excluded by tissue autopsy (Engel et al., 2011; Yu et al., 2011).

Neurological evaluation

Garcia behavioral scores (Garcia et al., 1995) were used to assess the rats' neurological deficits on parameters including spontaneous activity, symmetry in the movement of four limbs, forepaw outstretching, climbing, body proprioception, and vibrissae touch. The rats were evaluated at 1, 2, and 3 days after surgery by an observer who was blinded to the group assignment. At each time point, two rats were neurologically evaluated from the sham group; eight rats were used from each of the Sevo and ischemia groups. The ARRIVE guidelines were complied with and the rats were evaluated with Garcia scores and then sacrificed by decapitation.

TTC staining

On day 1 and day 3 after surgery, rats were intraperitoneally anesthetized with 40 mg/kg ketamine and decapitated. Brains were removed quickly and 2-mm coronal sections from rostral to bregma were stained with 1% TTC (Sigma-Aldrich, St. Louis, MO, USA) for 5 minutes at room temperature. The brain sections stained with TTC were post-fixed in 4% paraformaldehyde overnight. TTC stained and fixed brain sections were photographed with an iPhone5 (Apple Inc., Cupertino, CA, USA) and analyzed with ImageJ software (http://imagej.net). The ischemic lesion was traced in each slice, and total infarct volume of rat brains was measured as described previously (Swanson and Sharp, 1994): (contralateral hemisphere volume – non-lesion ipsilateral hemisphere volume) / contralateral hemisphere volume × 100%. At each time point, we used two rats for TTC staining in the sham group, and eight rats in both the Sevo and ischemia groups.

Brain section preparation

Rats were deeply anesthetized with 40 mg/kg ketamine *via* intraperitoneal injection and decapitated on the allocated day of the experiment. The brain tissues were fixed with 4% paraformaldehyde, and subsequently dehydrated with 30% sucrose in 0.1 M phosphate buffered saline (PBS) for 24 hours at 4°C. Afterwards, the dehydrated tissues were embedded in Tissue-Tek optimal cutting temperature compound (Sakura Finetek Inc., Nagano, Japan) for 30 minutes at −20°C and cut into coronal sections (45 μm thickness) on a freezing microtome (Leica CM 900; Leica, Nussloch, Germany). Floating

brain sections were preserved in the cryoprotectant (30% sucrose + 30% glycol in the PBS buffer) for further use.

Immunostaining

Brain sections were washed in 0.1 M PBS for 15 minutes and incubated with blocking solution (0.2% Triton X-100 and 10% donkey serum in 0.1 M PBS) for 60 minutes at room temperature. Sections were incubated with primary antibodies (**Table 1**) in dilute solution (0.2% Triton X-100 and 5% goat serum in 0.1 M PBS) overnight at 4°C, and then incubated with secondary antibodies (1:1000; Jackson, West Grove, PA, USA) for 2 hours at room temperature. Glial fibrillary acidic protein (GFAP) was used to label astrocytes, ionized calcium binding adaptor molecule-1 (Iba-1) for microglial cells, microtubule-associated protein 2 (MAP2) for neurons, doublecortin (DCX) for neuroblasts, NF-70 for neurofilaments and Ki67 for cell proliferation, respectively. Nuclei were counterstained by 4′,6-diamidino-2-phenylindole (DAPI). All images were scanned with Leica SP8 (Leica Microsystems Inc., Buffalo Grove, IL, USA) or Zeiss LSM 710 (Carl Zeiss MicroImaging GmbH, Jena, Germany) confocal microscopes with Z-stacks. The stitching pictures were constructed by 20 μm-thick Z-stacks (5 μm per step) with 20× oil immersion. All the image stacks were processed by ImageJ software and Adobe Photoshop CS6 (Adobe Systems Inc., San Jose, CA, USA). Nuclear morphology was used to identify the boundary of the infarct with dotted lines (Clarke, 1990). The cellular nuclei of non-infarct present as normal or pyknotic (early-stage apoptosis). The nuclei of the infarct present with karyorrhexis, which indicate that the dying cells are undergoing necrosis and late-stage apoptosis. Given that all the neural nuclei can be dyed with DAPI, the microglial cells with $DAPI^+$ debris engulfment were used to assist the delineation of the infarcted edge (Li et al., 2017). At each time point, there were eight rats in each group.

Statistical analysis

The statistical analyses were performed with GraphPad Prism 5 (GraphPad Software, San Diego, CA, USA). All values except neurological functional data were expressed as the mean ± SEM and analyzed by an unpaired Student's *t*-test or one-way analysis of variance with Bonferroni correction. In all cases, $P < 0.05$ was considered statistically significant.

Results

Sevoflurane preconditioning reduces cerebral infarct volume and improves neurological outcome in I/R rats

TTC staining and Garcia behavior scores were utilized to investigate the neuroprotection of sevoflurane preconditioning against cerebral I/R injury in rats. Our TTC staining results showed that the infarct volumes of the Sevo group were significantly reduced on day 3 after injury compared with the ischemia group ($P < 0.05$; **Figure 1A, B**). The neurological behavior scores of sevoflurane preconditioned rats were significantly higher than those in the ischemia group from day 1 to day 3 after injury ($P < 0.05$; **Figure 1C**).

Sevoflurane preconditioning accelerates astrocytic dynamics accompanied by microglia activation in I/R rats

The spatial and temporal dynamics of astrocytic cells were observed from day 1 to day 28 after ischemic injury. Our current data showed that the $Iba\text{-}1^+$ microglia were dramatically activated and migrated to the infarct from day 3 after I/R in rats with sevoflurane preconditioning. However, the microglial activation was postponed until day 7 in the ischemia group (**Figure 2A**). Coincidentally, migration of reactive astrocytes with typical long processes towards infarct areas occurred significantly earlier in the Sevo group (from day 3) than that in the ischemia group (not until day 7 after ischemia). On day 14, reactive astrocytes covered the whole infarcted areas and built up astrocytic networks in the Sevo group. However, many astrocytes were obstructed and confined within the thick astrocytic scars around the lesion sites in the rats without sevoflurane preconditioning (**Figure 2A** and **C**). Astrocytic migrating distances were calculated and compared among the two groups from day 1 to day 28 after I/R injury. The distance was defined as the length from the dotted line to the furthest protruding extension of astrocytic processes. The mean astrocytic migrating distance of the Sevo group was significantly greater than that of the ischemia group from day 3 to day 28 after injury ($P < 0.05$; **Figure 2B**).

Sevoflurane preconditioning promotes neuroblast migration facilitated by astrocytic scaffolds

We calculated and compared the number of neuroblasts, marked with DCX, in the ipsilateral subventricular zone (SVZ) between two groups on day 14 after I/R injury. Neuroblast proliferation was identified with Ki67, the recognized

Table 1 Primary antibodies used in this study

Antibody	Isotype	Dilution	Source (product No.)
Iba-1	Goat IgG	1:1000	Abcam, Cambridge, MA, USA (ab5076)
GFAP	Mouse IgG	1:1000	Abcam (ab10062)
GFAP	Rabbit IgG	1:5000	Abcam (ab7260)
MAP2	Rabbit IgG	1:1000	Abcam (ab32454)
DCX	Goat IgG	1:250	Santa Cruz, Dallas, Texas, USA (sc8066)
NF-70	Mouse IgG	1:1000	Millipore, Darmstadt, Germany (mab1615)
Ki67	Rabbit IgG	1:100	Abcam (ab15580)
DAPI	Rabbit IgG	1:10000	Abcam (ab104140)

Iba-1: Ionized calcium binding adaptor molecule-1; GFAP: glial fibrillary acidic protein; MAP2: microtubule associated protein 2; DCX: doublecortin; NF-70: neurofilament-70 kDa; DAPI: 4',6-diamidino-2-phenylindole.

marker for cellular proliferation. The migratory neuroblasts were characterized by the typical morphology of DCX^+ cells with long, bipolar or unipolar processes (Arvidsson et al., 2002; Taylor et al., 2016). Sevoflurane preconditioning markedly increased the DCX^+ cells in the ipsilateral SVZ (**Figure 3A**), including the total, proliferative ($DCX^+/Ki67^+$) and the migratory DCX^+ number ($2.01 \pm 0.44 \times 10^5/mm^3$, $4.4 \pm 0.17 \times 10^4/mm^3$, and $7.4 \pm 2.5 \times 10^4/mm^3$ respectively), compared with the ischemia group ($0.37 \pm 0.04 \times 10^5/mm^3$, $0.73 \pm 0.09 \times 10^4/mm^3$, $0.5 \pm 0.06 \times 10^4/mm^3$, $P < 0.05$, respectively) (**Figure 3B**). In addition, quantities of organized astrocytic scaffolds were observed to link the SVZ towards infarct region in the Sevo group on day 14. Compared with the ischemia group, a large number of DCX^+ cells were either embedded in astrocytic processes or in close contact with them, and the neuroblast streams had definitely formed and developed from SVZ to the infarct region in the Sevo group on day 14 (**Figure 3C**).

Sevoflurane preconditioning promotes neural networks formation following astrocytic activation

To investigate the formation of neural networks in the infarcted lesions, we used triple immunostaining to observe the distribution of neurons, astrocytes and microglial cells

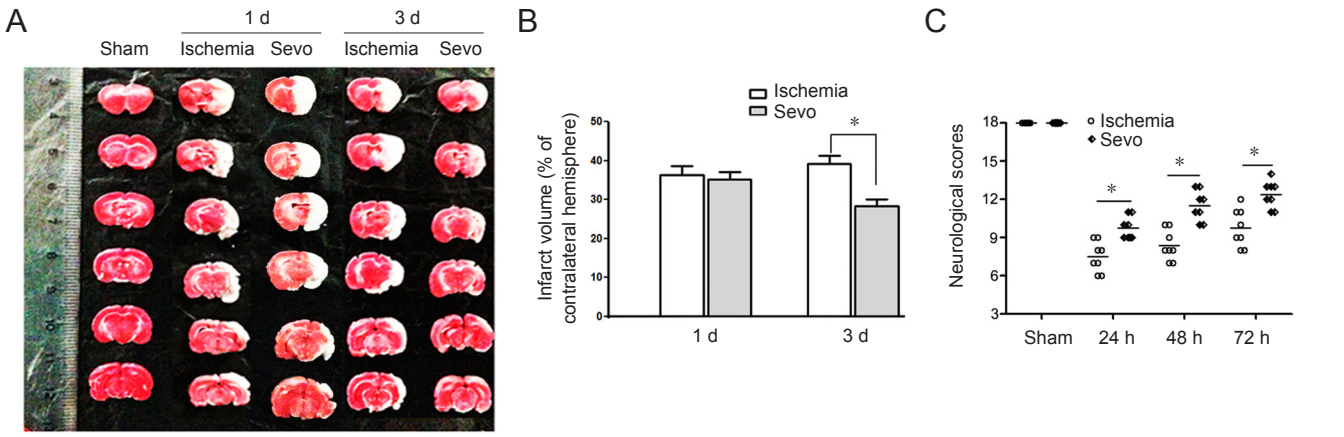

Figure 1 Sevoflurane preconditioning decreases infarct volumes and improves the neurological behavior of rats following cerebral ischemia and reperfusion.

(A) Representative brain slices stained with TTC on days 1 and 3 after ischemia/reperfusion. (B) Histogram comparison of infarct volumes between the ischemia and Sevo groups on days 1 and 3 after ischemia and reperfusion. Data are expressed as the mean ± SEM ($n = 8$ for Sevo and ischemia groups at each time point; Student's *t*-test). $*P < 0.05$. (C) Scattergram comparison of Garcia's neurobehavioral scores among the sham, ischemia and Sevo groups at 24, 48, and 72 h after injury. All scores were expressed as the median ($n = 8$ for Sevo and ischemia groups at each time point, and $n = 2$ for the sham group; one-way analysis of variance with Bonferroni correction). $*P < 0.05$. Sevo: Sevoflurane; TTC: 2,3,5-triphenyltetrazolium chloride; d: day(s); h: hours.

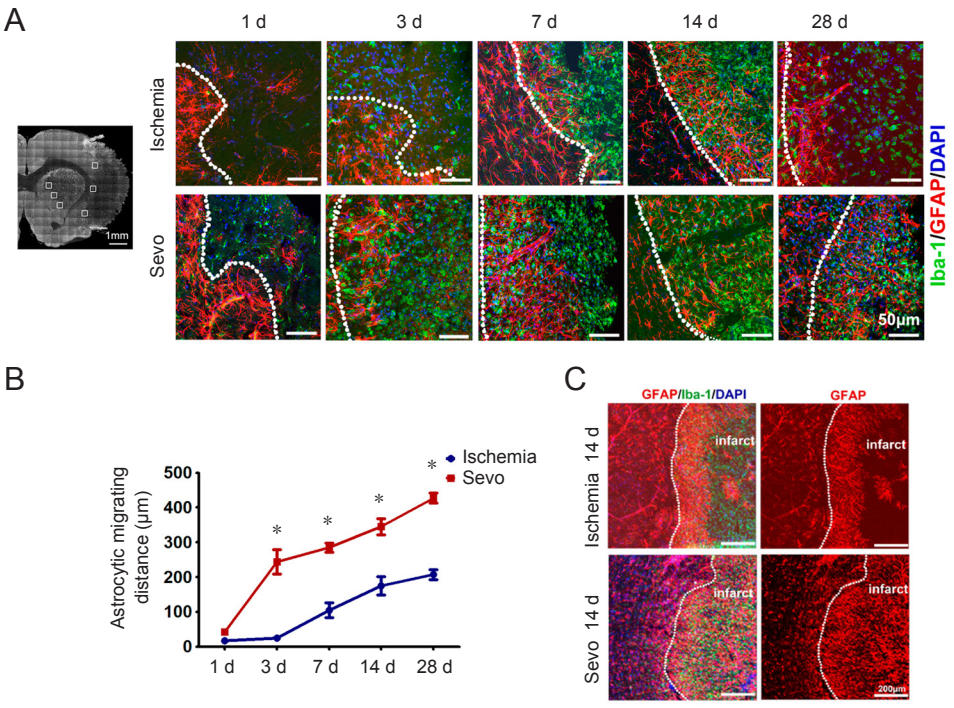

Figure 2 Sevoflurane preconditioning accelerates astrocytic dynamics accompanied with microglial activation in rats following cerebral ischemia and reperfusion.

(A) Migration patterns of microglia and astrocytes into the infarct in the brain of rats in the Sevo and ischemia groups on days 1, 3, 7, 14 and 28. Boxed areas of the black-and-white stitching image (with scale bar: 1 mm) indicate magnified peri-ischemia regions of cortex and striatum in the right panels. Three coronal sections per rat, with three different regions of peri-infarcted cortex and striatum per section, were used to calculate astrocytic migrating distance. Scale bar: 50 μm. (B) Comparison of the astrocytic migrating distance on days 1, 3, 7, 14 and 28 after ischemia/reperfusion injury. Data are expressed as the mean ± SEM ($n = 8$; one-way analysis of variance with Bonferroni correction). $*P < 0.05$, *vs.* ischemia group. (C) Comparison of astrocytic scars between two groups on day 14 after injury. Scale bars: 200 μm. Dotted lines indicate lesion borders in A and C. Sevo: Sevoflurane; DAPI: 4′,6-diamidino-2-phenylindole; GFAP: glial fibrillary acidic protein; d: day(s).

on day 7 and 14 after I/R injury. In the ischemic lesions, MAP2$^+$ neurons of the Sevo group appeared with neuron axons beyond the microglial somas from day 7, which indicated the survival of newborn neurons. On day 14 it was noted that the closer to the edge of infarct lesion, the more MAP2$^+$ cells were observed (**Figure 4A**). In the infarcted area, the number of MAP2$^+$ neurons in the Sevo group was nearly three times higher than that of the ischemia group on day 14 after injury (**Figure 4B**). In addition, neuronal and glial networks, closely resembling those of the normal brain, were observed to have been rebuilt with NF-70$^+$ neurofilaments, GFAP$^+$ astrocytes and Iba1$^+$ microglial cells in rats with sevoflurane preconditioning on day 14 after I/R injury (**Figure 4C**).

Discussion

There is growing evidence that astrocytes and numerous gli-

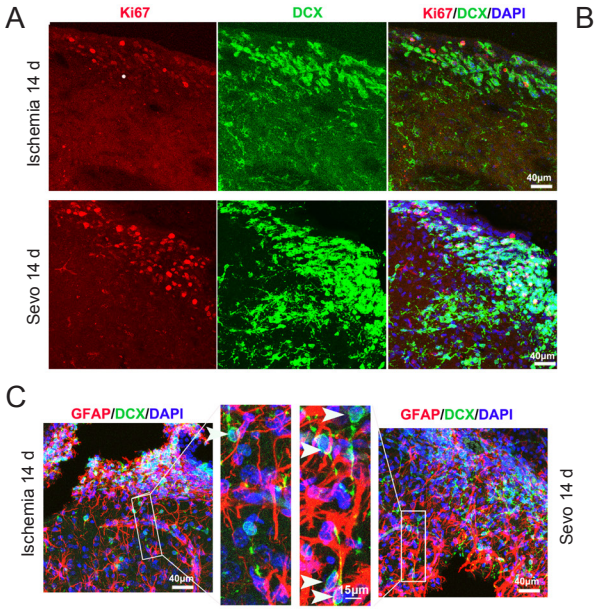

Figure 3 Sevoflurane preconditioning promotes neuroblast migration with astrocytic scaffolds in rats following cerebral ischemia and reperfusion.
(A) Representative images showing the proliferation (Ki67$^+$) of neuroblasts (DCX$^+$) in the ipsilateral subventricular zone on day 14 after ischemia/reperfusion injury, which indicate that Sevo preconditioning promotes the neuroblast proliferation in subventricular zone. Scale bars: 40 μm. (B) Comparison of DCX$^+$ cell number in the ipsilateral subventricular zone between the two groups on day 14. Number of DCX$^+$ cells in boxed areas was calculated and expressed as the mean ± SEM (n = 8; one-way analysis of variance with Bonferroni correction). *P < 0.05. (C) Representative images showed the astrocytic scaffolds (GFAP$^+$) for neuroblasts (DCX$^+$) migration in the two groups. More astrocytic scaffolds (arrowheads) were observed in the Sevo group on day 14 after injury. Boxed area showed magnified region (scale bar: 15 μm). Scale bars: 40 μm. Sevo: Sevoflurane; DAPI: 4′,6-diamidino-2-phenylindole; GFAP: glial fibrillary acidic protein; DCX: doublecortin.

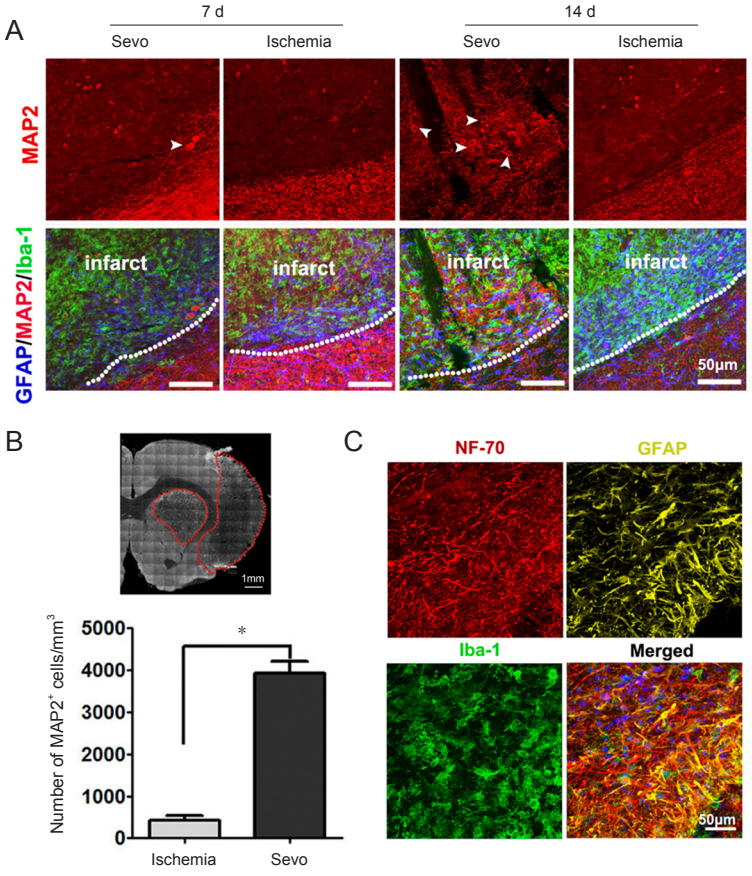

Figure 4 Sevoflurane preconditioning enhances neural network formation in the infarct brain region of rats after stroke.
(A) Representative images showing the neurons (MAP2$^+$), astrocytes (GFAP$^+$) and microglial cells (Iba-1$^+$) in the infarct region in both groups on days 7 and 14 after ischemia/reperfusion injury. More MAP2$^+$ neurons were observed in the infarct areas of the Sevo group than the ischemia group. Dotted lines indicate margin of the infarct; white arrows show the newly formed neurons. (B) MAP2$^+$ cell number in the infarct on day 14 after ischemia/reperfusion injury. Red dotted lines delineate the boundary of the infarct. The data are expressed as the mean ± SEM (n = 8; Student's t-test). *P < 0.05. (C) Representative images show the reconstruction of neurofilaments (NF-70$^+$), astrocyte (GFAP$^+$), microglia (Iba-1$^+$) network, separately and merged, in the infarct with Sevo preconditioning. Scale bar: 50 μm. Sevo: Sevoflurane; MAP2: microtubule-associated protein 2; GFAP: glial fibrillary acidic protein; NF: neurofilament; Iba-1: ionized calcium binding adaptor molecule-1.

al cells in the central nervous system are crucially involved in stroke, with beneficial or detrimental aspects at different stages (Anderson et al., 2003; Huang et al., 2018). In the acute ischemic stage astrocytes are activated immediately, enabling the synthesis and release of cytokines and chemokines, initiating inflammatory cascades that might exacerbate secondary brain damage (Zhang et al., 2017). Reactive astrocytes establish a glial scar that limits the spread of inflammatory cytokines and apoptotic messengers to healthy regions. Neurotrophins, such as brain-derived neurotrophic factor, nerve growth factor and basic fibroblast growth factor, are synthesized and released by astrocytes to enable the brain repairing processes (Martin et al., 2013). These ambivalent characteristics of astrocytes prompted our investigation into the impact of sevoflurane preconditioning on the spatial (from penumbra to ischemic core region) and temporal dynamics (from day 1 until day 28 after stroke) of reactive astrocytes. To our knowledge, few studies have focused on the astrocytic dynamics in the mechanism of neuroprotection by inhalational anesthetics. We found many reactive astrocytes ($GFAP^+$) with typical long processes migrated towards the infarct lesions from day 3 after I/R injury in the Sevo group. However, few astrocytes were activated and migrated to ischemic insults until day 7 in the ischemia group. These findings were consistent with the data of a previous study (Panickar and Norenberg, 2005). The measurement and comparison of astrocytic migrating distance gives further support for sevoflurane preconditioning accelerating the astrocytic activation and migration to the infarct in the acute ischemic stage. In the present study, we did not investigate and compare the astrocytic proliferation between the two groups after stroke was induced. Li et al. (2014) demonstrated that there was an increase of proliferating reactive astrocytes in a time-dependent manner after stroke, but the proliferating reactive astrocytes only account for a small portion of the total proliferating cells.

Astrogliosis and glial scar formation are some of the prominent features of cerebral ischemic injury. The reactive astrocytes restrict inflammatory cascades and secondary brain damage by building up a glial scar around the infarct lesions after brain ischemia. The formation of a glial scar in the peri-infarct region demarcates the ischemic region from healthy tissue with dominant astrocytic morphological changes and proliferation (Sofroniew and Vinters, 2010). However, recent studies have found that peri-infarct astrogliosis, acts as a barrier, impeding the neurogenesis and reconstruction in the late recovery stage (Yuan et al., 2015; Sims and Yew, 2017). In the present study, accumulation of astrocytes formed scar-like barriers around the edge of the peri-infarct regions from day 14 after brain ischemia in the ischemia group. In contrast, astrocytic networks had been established and covered the whole infarct by the same time point in the Sevo group. The difference in microglial activation might explain this phenomenon. The present data is consistent with our previous finding that Sevoflurane preconditioning accelerated microglial activation prior to astrocytic activation after brain ischemia (Li et al., 2017). Activated microglial cells exert phagocytosis by clearing up neural debris in the infarct region. Without the obstacle of cellular debris, astrocytes in the Sevo group migrated directly towards the ischemic core and established astrocytic networks by day 14 after ischemic insults. In contrast, astrocytes without sevoflurane pretreatment were obstructed by the remains of neural debris that accumulated at the border of the ischemic lesions, inhibiting the post-injury repair progress.

Astrocytes are known to provide metabolic, trophic and structural support to neurons and vasculature by wrapping or ensheathing synapses and blood vessels (Sofroniew and Vinters, 2010). In the present study, we also identified an important role that astrocytic scaffolds play in neurogenesis and reconstruction after stroke. This is consistent with a previous study (Anderson et al., 2003). In the Sevo group, the astrocytic networks provided structural scaffolds for neuroblasts (DCX^+) migrating from the SVZ to the ischemic core region, and established neuron-neuroglia networks from day 14 after stroke. However, few neuroblasts (DCX^+/$Ki67^+$) and newborn neurons ($MAP2^+$) were observed in the ischemic regions of untreated brains. Young et al. (2013) pointed out that hypertrophic reactive astrocytes with tortuous processes disrupted the neuroblast migratory scaffold and thus impeded neural recovery after stroke. Hayakawa et al. (2010) demonstrated that inhibition of reactive astrocytes by fluorocitrate could decelerate neurovascular recovery after focal brain ischemia in mice. These previous studies are consistent with our results that sevoflurane preconditioning promotes the formation of astrocytic bridges, which facilitate neuroblasts migrating to ischemic lesions.

There are some limitations to this study. First, GFAP, a 'pan-astrocyte' marker, was utilized to label prototypic astrocytic dynamics. The expression levels of GFAP are shown to be different in fibrous astrocytes and protoplasmic astrocytes. Aldh1L1, a homogenously expressed astrocyte specific protein, might be an optimal marker to label the reactive astrocytes (Cahoy et al., 2008). Second, the spatial and temporal dynamics of astrocytic cells were observed with immunostaining in wildtype rats. Due to astrocytic heterogeneity in the central nervous system (Benesova et al., 2009), accurate and detailed investigation of astrocytic dynamics might be optimally performed with transgenic mice expressing astrocytic fluorescent marker. Third, reactive astrocytes have been indicated to exhibit stem cell-like properties (Dimou and Götz, 2014). In our previous study, we demonstrated that sevoflurane preconditioning accelerated neuroblasts to differentiate into neurons, astrocytes and oligodendrocytes after brain ischemia (Li et al., 2017). Further study will be required to identify whether sevoflurane preconditioning confers neurogenesis *via* promoting reactive astrocytes differentiating into neurons. Lastly, astrogliosis has been demonstrated to play a pivotal role in neuroinflammation contributing to Alzheimer's disease and postoperative cognitive dysfunction (Ologunde and Ma, 2011; Lyman et al., 2014). Regarding the dual function of reactive astrocytes on both neuroprotection and neurotoxicity, we should be cautiously optimistic about glial cell-based therapy, and perform further studies to clarify the astrocytic roles in neural diseases.

In summary, sevoflurane could effectively prevent brain

against ischemic injury, partly by accelerating astrocytic activation and migration, facilitating the formation of astrocytic scaffolds for neuroblasts migrating to ischemic lesions, and promoting the establishment of neural network in the infarct region after I/R injury. Our results contribute to establishing the neuroprotective mechanism of sevoflurane and possible astrocyte-based therapies in ischemic stroke.

Acknowledgments: *The authors wish to thank Professor Li-Xiang Ma and Hexige Saiyin for excellent technical assistance in confocal microscopy.*
Author contributions: *Study design: QY and WML; acquisition and analysis of data and images: LL and QY; paper writing and revision: QY, LL and WML. All authors approved the final version of the paper.*
Conflicts of interest: *None declared.*
Financial support: *The study was supported by the National Natural Science Foundation of China, No. 81200937. The funder had no involvement in the study design; data collection, management, analysis, and interpretation; paper writing; or decision to submit the paper for publication.*
Institutional review board statement: *All procedures were approved by the Animal Ethics Committee of Fudan University, China (2017 Huashan Hospital JS-003) on January 4, 2017 and performed in accordance with the National Institutes of Health Guide for the Care and Use of Laboratory Animals (NIH Publication No. 85-23, revised 1996).*

Data sharing statement: *Datasets analyzed during the current study are available from the corresponding author on reasonable request.*
Plagiarism check: *Checked twice by iThenticate.*
Peer review: *Externally peer reviewed.*

Open peer reviewers: *Jing Chen, Jining Medical University, China; Min Cheol Chang, Asan Medical Center, Republic of Korea.*
Additional file: *Open peer review reports 1 and 2.*

References

Anderson MF, Blomstrand F, Blomstrand C, Eriksson PS, Nilsson M (2003) Astrocytes and stroke: networking for survival? Neurochem Res 28:293-305.
Arrowsmith JE, Grocott HP, Reves JG, Newman MF (2000) Central nervous system complications of cardiac surgery. Br J Anes 84:378-393.
Arvidsson A, Collin T, Kirik D, Kokaia Z, Lindvall O (2002) Neuronal replacement from endogenous precursors in the adult brain after stroke. Nat Med 8:963-970.
Benesova J, Hock M, Butenko O, Prajerova I, Anderova M, Chvatal A (2009) Quantification of astrocyte volume changes during ischemia in situ reveals two populations of astrocytes in the cortex of GFAP/EGFP mice. J Neurosci Res 87: 96-111.
Cahoy J, Emery B, Kaushal A, Foo L, Zamanian J, Christopherson K, Xing Y, Lubischer J, Krieg P, Krupenko S, Thompson W, Barres B (2008) A transcriptome database for astrocytes, neurons, and oligodendrocytes: a new resource for understanding brain development and function. J Neurosci 28:264-278.
Chen Y, Nie H, Tian L, Tong L, Deng J, Zhang Y, Dong H, Xiong L (2015) Sevoflurane preconditioning-induced neuroprotection is associated with Akt activation via carboxy-terminal modulator protein inhibition. Br J Anaesth 114:327-335.
Clarke P (1990) Developmental cell death: morphological diversity and multiple mechanisms. Anat Embryol 181:195-213.
Dimou L, Götz M (2014) Glial cells as progenitors and stem cells: new roles in the healthy and diseased brain. Physiol Rev 94:709-737.
Engel O, Kolodziej S, Dirnagl U, Prinz V (2011) Modeling stroke in mice – middle cerebral artery occlusion with the filament model. J Vis Exp 47:e2423.
Garcia J, Wagner S, Liu K, Hu X (1995) Neurological deficit and extent of neuronal necrosis attributable to middle cerebral artery occlusion in rats. Statistical validation. Stroke 26:627-634.
Han J, Zhang JZ, Zhong ZF, Li ZF, Pang WS, Hu J, Chen LD (2018) Gualou Guizhi decoction promotes neurological functional recovery and neurogenesis following focal cerebral ischemia/reperfusion. Neural Regen Res 13:1408-1416.
Hayakawa K, Nakano T, Irie K, Higuchi S, Fujioka M, Orito K, Iwasaki K, Jin G, Lo E, Mishima K, Fujiwara M (2010) Inhibition of reactive astrocytes with fluorocitrate retards neurovascular remodeling and recovery after focal cerebral ischemia in mice. J Cereb Blood Flow Metab 30:871-882.
Huang Y, He J, Xiang Y, Wang ZQ, Du G, Wang QS (2018) Changes of perivascular astrocyte foot process in the cerebral cortex of a mouse model of sustained hyperglycemia. Zhongguo Zuzhi Gongcheng Yanjiu 22:3218-3223.
Li H, Zhang N, Lin H, Yu Y, Cai Q (2014) Histological, cellular and behavioral assessments of stroke outcomes after photothrombosis-induced ischemia in adult mice. BMC Neurosci 15:58.
Li L, Saiyin H, Xie J, Ma L, Xue L, Wang W, Liang W, Yu Q (2017) Sevoflurane preconditioning induced endogenous neurogenesis against ischemic brain injury by promoting microglial activation. Oncotarget 8:28544-28557.
Liu Z, Chopp M (2016) Astrocytes, therapeutic targets for neuroprotection and neurorestoration in ischemic stroke. Prog Neurobiol 144:103-120.
Lyman M, Lloyd D, Ji X, Vizcaychipi M, Ma D (2014) Neuroinflammation: The role and consequences. Neurosci Res 79:1-12.
Maki T, Hayakawa K, Pham L, Xing C, Lo E, Arai K (2013) Biphasic mechanisms of neurovascular unit injury and protection in CNS diseases. CNS Neurol Disord Drug Targets 12:302-315.
Martin J, Magistretti P, Allaman I (2013) Regulation of neurotrophic factors and energy metabolism by antidepressants in astrocytes. Curr Drug Targets 14:1308-1321.
Ologunde R, Ma D (2011) Do inhalational anesthetics cause cognitive dysfunction? Acta Anaesthesiol Taiwan 49:149-153.
Panickar K, Norenberg M (2005) Astrocytes in cerebral ischemic injury: morphological and general considerations. Glia 50:287-298.
Sims NR, Yew WP (2017) Reactive astrogliosis in stroke: Contributions of astrocytes to recovery of neurological function. Neurochem Int 107:88-103.
Sofroniew M, Vinters H (2010) Astrocytes: biology and pathology. Acta Neuropathol 119:7-35.
Swanson RA, Sharp FR (1994) Infarct measurement methodology. J Cereb Blood Flow Metab 14:697-698.
Taylor S, Smith C, Keeley K, McGuone D, Dodge C, Duhaime A, Costine B (2016) Neuroblast distribution after cortical impact is influenced by white matter injury in the immature gyrencephalic brain. Front Neurosci 10:387.
Wang H, Lu S, Yu Q, Liang W, Gao H, Li P, Gan Y, Chen J, Gao Y (2011) Sevoflurane preconditioning confers neuroprotection via anti-inflammatory effects. Front Biosci (Elite Ed) 3:604-615.
Wang Q, Xiong L, Chen S, Liu Y, Zhu X (2005) Rapid tolerance to focal cerebral ischemia in rats is induced by preconditioning with eletroacupuncture: window of protection and the role of adenosine. Neurosci Lett 381:158-162.
Wang W, Jiang B, Sun H, Ru X, Sun D, Wang L, Wang L, Jiang Y, Li Y, Wang Y, Chen Z, Wu S, Zhang Y, Wang D, Wang Y, Feigin V; NESS-China Investigators (2017) Prevalence, incidence, and mortality of stroke in China: results from a nationwide population-based survey of 480687 adults. Circulation 135: 759-771.
Wilson PV, Ammar AD (2005) The incidence of ischemic stroke versus intracerebral hemorrhage after carotid endarterectomy: a review of 2452 cases. Ann Vasc Surg 19:1-4
Young CC, van der Harg JM, Lewis NJ, Brooks KJ, Buchan AM, Szele FG (2013) Ependymal ciliary dysfunction and reactive astrocytosis in a reorganized subventricular zone after stroke. Cereb Cortex 23:647-659.
Yu Q, Wang H, Chen J, Gao Y, Liang W (2010) Neuroprotections and mechanisms of inhalational anesthetics against brain ischemia. Front Biosci (Elite Ed) 2:1275-1298.
Yu Q, Chu M, Wang H, Lu S, Gao H, Li P, Gan Y, Shi H, Liang W, Chen J, Gao Y (2011) Sevoflurane preconditioning protects blood-brain-barrier against brain ischemia. Front Biosci (Elite Ed) 3:978-988.
Yuan J, Zou M, Xiang X, Zhu H, Chu W, Liu W, Chen F, Lin J (2015) Curcumin improves neural function after spinal cord injury by the joint inhibition of the intracellular and extracellular components of glial scar. J Surg Res 195:235-245.
Zhang Y, Tian SY, Li YW, Zhang L, Yu JB, Li J, Chen YY, Wang YX, Liang Y, Zhang XS, Wang WS, Liu HG (2015) Sevoflurane preconditioning improving cerebral focal ischemia-reperfusion damage in a rat model via PI3K/Akt signaling pathway. Gene 569:60-65.
Zhang YK, Yang JH, Gao F, Duan FY (2017) Effect of Buyang Huanwu decoction combined with bone marrow mesenchymal stem cell transplantation on expression of integrin in a rat model of middle cerebral artery occlusion. Zhongguo Zuzhi Gongcheng Yanjiu 38:724-729.

P-Reviewers: Chen J, Chang MC; C-Editor: Zhao M; S-Editor: Li CH; L-Editors: Qiu Y, Song LP; T-Editor: Liu XL